RSC Advances

ROYAL SOCIETY OF CHEMISTRY

www.rsc.org/advances

Micro-wheels Composed of Self-Assembled Tungsten Oxide Nanorods for Highly Sensitive Detection of Low Level Toxic Chlorine Gas

Pham Van Tong[1,2], Nguyen Duc Hoa[1]*, Nguyen Van Duy[1], Nguyen Van Hieu[1]*

[1]International Training Institute for Materials Science (ITIMS), Hanoi University of Science and Technology (HUST), Dai Co Viet, Hanoi, Vietnam

[2]Department of Physics, Faculty of Mechanical Engineering, National University of Civil Engineering (NUCE), No. 55, Giai Phong Str., Hanoi, Viet Nam

Corresponding authors

*** Nguyen Duc Hoa, Ph.D.**

*** Nguyen Van Hieu, Ph.D.**

Associate Professor

International Training Institute for Materials Science (ITIMS),

Hanoi University of Science and Technology (HUST)

No.1, Dai Co Viet Road, Hanoi, Vietnam

Phone: 84 4 38680787

Fax: 84 4 38692963

E-mail: ndhoa@itims.edu.vn ; hieu@itims.edu.vn

Post address: No.1 Dai Co Viet, Hanoi, Vietnam

Abstract: Micro-wheels about 7 μm in average diameter and 2.5 μm thick were formed by the self-assembly of tungsten oxide nanorods about 1.5 μm long and 10 nm in diameter. The micro-wheels were hydrothermally synthesized for the ppt level monitoring of highly toxic chlorine (Cl_2) gas. The gas sensor based on the fabricated micro-wheels showed excellent performance within a wide range of Cl_2 concentration (100 ppb to 500 ppb), having a high response of ~10- to 25-fold. This sensor also had an ultra-low detection limit of ~18 ppt, which was significantly lower than its permissive environmental concentration. In addition, the transient stability of the sensor even after five cycles of switching on/off from air-to-gas demonstrated effective reusability of the device.

Keywords: Micro-wheel, tungsten oxide nanorod, Cl_2 gas sensor

1. Introduction

Chlorine (Cl_2) is an oxidizing gas commonly used as an effective whitener and disinfector in many industrial processes. It is an environmentally harmful gas with a distinctive smell of a pepper–pineapple mixture and can be used as a chemical weapon. [1] The human nose can distinguish the smell of Cl_2 gas in the concentration range of 0.1 – 0.3 ppm, but this level is considerably higher than its permissive environmental concentration at workplace of approximately 0.034 ppm, while the long-term exposure limit (6-hour exposures) is 0.5 ppm. [2] Inhaling Cl_2 gas at low concentration of approximately 30 ppm can cause coughing and vomiting. [2] Therefore, developing a highly sensitive gas sensor for the detection of Cl_2 gas at the ppb or ppt level is highly important in environmental monitoring and safety use. [1,3]

Tungsten oxide, a wide band gap n-type transition metal oxide, has attracted increasing attention in recent years because of its outstanding physicochemical properties and tremendous capacity to sense different gases. [4] Tungsten oxide nanorods [5] and nanowires [6] have been used for gas sensing applications because of their high surface-to-volume ratio, quantum confinement effects [7], and high sensitivity. [8] This high sensitivity is ascribed to the compatibility of crystalline size and Debye length. The assembly of nanostructures into building blocks and/or porous structured materials has also been gaining increasing interest as a powerful technique to integrate various nanomaterials into macroscopic structures or devices.[9,10] In addition, the assembly of nanorods into porous structures reportedly shows a satisfactory gas sensing performance because of their 3D network and high effective surface area [11,12], which provide large active surface sites for gas adoption and accelerate the gas diffusion rate. [13] Wang et al. [14] prepared hierarchically assembled tungsten oxide (hydrates) nano/microstructures by crystal-seed-assisted hydrothermal process, where they could obtain different morphologies such as double layer nano/microbundles, quasi-

nanorod arrays, nanorod-spheres, double-layer nano/microdisks and double-layer six-pod prisms. Xu et al. [15] prepared tungsten oxide with three-dimensional flower-like and wheel-like architectures by hydrothermal method, where they varied the pH of the precursor solution to obtain different morphologies. The 3D configuration with large void space can provide large surface area for enhanced photo-catalytic activity. [15] This characteristic is also expected to enhance the gas sensing characteristics of materials. However, micro-wheels composed of self-assembled tungsten oxide nanorods have yet to be synthesized for gas sensing applications. In addition, the fabrication of a highly sensitive and low-cost Cl_2 sensor at the ppb or ppt level remains challenging.

Herein, micro-wheels composed of self-assembled tungsten oxide nanorods were hydrothermally synthesized for the ppt level detection of highly toxic Cl_2 gas. The design of gas nanosensor based on micro-wheels made of self-assembled tungsten oxide nanorods is shown in Figure 1, which involves the micro-wheels of tungsten oxide deposited on a pair of interdigitated Pt electrodes. The synthesis of micro-wheels is based on the in situ growth and self-assembly of the nanorods under acidic conditions, with pluronic (P123) as a structure-directing agent. The obtained tungsten oxide material shows excellent performance for Cl_2 gas sensing at a low concentration (100 ppb to 500 ppb) with a fast response and recovery. This excellent performance can be ascribed to the exceptional properties of the micro-wheel structure that provide the diffusion path for gas molecules to adsorb on the active sites and total depletion.

2. Experimental

Micro-wheels composed of self-assembled tungsten oxide nanorods were hydrothermally synthesized by using sodium tungstate hydrate, sodium chloride, and P123 as precursors. In a

typical synthesis, sodium tungstate hydrate (1.5 g), sodium chloride (0.5 g), and P123 surfactant (0.5 g) were dissolved in 80 mL of distilled water, and then the pH of the solution was adjusted to 2.5 by adding a sufficient amount of concentrated hydrochloric acid. This solution was poured into a Teflon-lined autoclave for hydrothermal reaction at 200 °C for 12 h. After cooling to room temperature, the precipitated products were collected by centrifugation at 4000 rpm. To remove the excess sodium salt and un-reacted compounds we washed the precipitated powders several times with distilled water and ethanol solution, and then re-centrifugation to collect the products. Finally, the collected products were air dried at 60 °C prior to being used in sensor fabrication and characterization. For sensor fabrication, 20 mg of the synthesized materials was gently dispersed in ethanol solution to obtain a colloidal solution of 4 mg/mL. Thereafter, the colloidal solution was dropped onto a thermally oxidized silicon substrate equipped with a pair of interdigitated Pt electrodes. The sensor chip substrate was prepared on a silicon wafer by using micro-electronic technology toward the mass production. Details about the micro-electronic fabrication process for sensor chip can be found elsewhere [16]. The as-obtained sensors were dried at room temperature for 24 h and then heat-treated at 600 °C/2 h to stabilize the sensor resistance. The gas sensors were measured by a flow-through technique with a standard flow rate of 400 sccm for dry air balance and analytic gases. Before measurement started, the dry air was flown through the sensing chamber until the resistance of the sensors stabilized. The gas-sensing chamber was designed as a black-box, thus environmental light was not influenced on the performance of derive. Details about the gas-sensing measurement system can be seen in Figure S1 (Supplementary). Herein, we used the standard gas concentration of 100 ppm Cl_2 balanced in nitrogen and mixed with dry air as carrier using a series of mass flow controllers to obtain a lower concentration. The gas concentration was calculated as follows:

$C(ppm)=C_{std}(ppm)\times f/(f+F)$, where f and F are the flow rates of analytic gas and dry air, respectively, and $C_{std}(ppm)$ is the concentration of the standard gas used in the experiment. During sensing measurement, the resistance of the sensors was continuously measured using a Keithley instruments (model 2602) interfaced with a computer while the dried air and analytic gases were switched on/off each cycle. [4]

3. Results and discussion

The morphology of the sensor chip fabricated on the silicon substrate is shown in Figure 2(A). The center of the sensor chip was isolated by silicon dioxide edge, which surrounded the sensing region. A micro heater and a micro thermocouple were integrated in the chip to provide heat energy, activate the sensing area, and measure the temperature. The morphology of the synthesized tungsten oxide material was characterized by FESEM, and the data are shown in Figures 2(B) and 2(C). The FESEM images revealed that the nanorods assembled to form micro-wheels with homogenous morphology. The formation of the micro-wheels is based on the aggregation mechanism. The dish-like materials were grown at the initial hydrothermal condition based on the Ostwald ripening mechanism and then the nanorods were grown and aggregated into the micro-wheels to reduce the free energy of the system. This result is consistent with other report. [15] The reproducibility of the hydrothermal process was also studied by repeating the experiment under a fixed condition. As can be seen in Figure S2 (Supplementary), the SEM images indicate that the obtained products have a similar morphology, indicating a good reproducibility of the synthesis. The HRTEM image showed that the nanorods were highly crystalline and that lattice fringes can be clearly observed (Figure 2(D)). The interspace of the lattice fringes was approximately 0.39 nm, which was consistent with the gap between (001) planes of hexagonal WO_3 (JCPDS, 33-1387). The XRD pattern of the synthesized tungsten oxide

shown in Figure S3 (Supplementary) indicated that the material had a hexagonal crystal structure (space group P6/mmm) with lattice parameters $a = b = 0.7298$ nm and $c = 0.3899$ nm (JCPDS, 33-1387). The strong and sharp diffraction peaks of the synthesized product confirmed the high crystallinity of the hexagonal tungsten oxide. The EDS analysis of the sample confirmed the presence of O and W, which originated from the tungsten oxide (Figure S4, Supplementary). EDS analysis was performed to estimate the composition of the micro-wheels. Results showed the deficiency of oxygen in the standard formula of $WO_{3-\sigma}$. The Raman spectrum of the as-synthesized tungsten oxide micro-wheels exhibited two strong W-O-W stretching modes at 804 and 713 cm^{-1} of WO_3 (Figure S5, Supplementary) and the bending modes of the bridging oxygen at 262 and 326 cm^{-1}. The lattice vibration mode of the crystalline WO_3 at 130 cm^{-1} also appeared in the Raman spectra. The photoluminescence spectrum (Figure S6, Supplementary) of the synthesized tungsten oxide showed a strong peak centered at 448 nm (2.77 eV) because of the localized state induced by the presence of oxygen vacancies and/or defects in the crystal of tungsten oxide. The strong luminescence of the synthesized tungsten oxide can also be ascribed to the quantum effect and/or a high level oxygen vacancy.

The transient resistance vs. time of the sensor measured at different temperatures upon exposure to given concentrations of Cl_2 gas is shown in Figure 3(A). The resistance of the sensor was approximately 109, 69, 58, and 23 kΩ when measured in air at 150 °C, 200 °C, 250 °C, and 300 °C, respectively. Upon exposure to 500 ppb Cl_2 gas, the resistance of the sensor rapidly increased and reached the saturation values of approximately 0.97, 1.83, 0.87, and 0.29 MΩ, respectively. The significant increase in sensor resistance upon exposure to the ppb level concentration of Cl_2 suggests that the materials are highly sensitive to oxidizing Cl_2 gas. As

demonstrated in the gas-sensing mechanism, [17] the oxidizing gas molecule was expected to adsorb at the terminal O or lattice O sites of metal oxide, capture the electron, form new surface states, and increase the resistance of the sensor. [18] This phenomenon is similar to that of NO_2 molecule adsorption on the surface of tungsten oxide. [19] Figure 3(B) shows sensor response (R_{gas}/R_{air}) as a function of Cl_2 concentrations measured at different temperatures. The sensor response clearly increased with increasing Cl_2 concentration at all measured temperatures. This result clearly indicated that the adsorption of gas molecules on the sensing layer surface did not yet reach saturation within 100 ppb to 500 ppb. The sensor exhibited the highest response to Cl_2 gas at 200 °C, revealing the moderate working temperature of the sensor. The sensor response (R_{gas}/R_{air}) to 100 ppb Cl_2 measured at 200 °C was approximately 10, which was 6.6-fold higher than that to 1 ppm Cl_2 (~1.5) of the mesoporous SnO_2. [20] However, this comparison needs precise control because the sensing performance is dependent on various parameters such as working temperature, sensor configuration, and etc. The results clearly indicated that the sensor can detect low gas concentrations. The detection limit, ***DL*** was calculated on the basis of the definition of IUPS as $\boldsymbol{DL}(ppb)=3(rms_{noise}/slope)$, where rms_{noise} is the root-mean-square deviation of gas response at the baseline and calculated as $rms_{noise} = \sqrt{\frac{\sum(S_i-S)^2}{N}}$, S_i is the experimental data points (10 points), and S is the corresponding values calculated from the fifth polynomial curve fitting. The rms_{noise} value was calculated to be 0.00023 ± 0.00008. The *slope* value was calculated to be 0.036 ± 0.008. Therefore, the ***DL***(ppb) value was observed to be approximately 0.018 ppb (or 18 ppt). This study is the first to obtain this ultra-low DL enabling the application of device in environmental monitoring of highly toxic Cl_2 gas at low concentration. The superior gas sensing characteristics of the self-assembled micro-wheels is possible due to the 3D configuration of materials that provide the large specific surface area and

abundant diffusion paths for gas molecules to adsorb on the active sites and totally depleted the nanorods, and thus improves the sensing performance. [12]

The reusability of the sensor was also considered for the real-time monitoring of Cl_2. Thus, the transient resistance vs. time of the sensor was tested to 250 ppb Cl_2 at 200 °C. Figure 3(C) shows the identically response characteristics to Cl_2 gas for the five cycles of measurement, indicating the good reusability of the sensor. The response of the sensor to reducing gas was also tested for NH_3 monitoring at different temperatures, and the data are presented in Figure 3(D). The transient resistance vs. time of the nanosensor upon exposure to different concentration of NH_3 measured at different temperatures is shown in Figure S7 (Supplementary). The response value to NH_3 was threefold smaller than that to Cl_2 gas even though the measured concentration range of NH_3 was threefold higher than that to Cl_2 gas. Figure S8 (Supplementary) shows the sensor response as a function of temperature (A) and as a function of NH_3 concentrations (B). The sensor also required a higher temperature (~400 °C) for optimal response to NH_3 gas, suggesting that the sensor can be used for the selective monitoring of Cl_2 in the interference of NH_3 at moderate temperature (~200 °C).

Not only application in Cl_2 gas sensor, the fabricated device could also be used as a light detector. As shown in Figure S9 (Supplementary), the I-V curves of the sensor measured at different temperatures in dark and under visible light irradiation. The electrical current of the device increased significantly when illuminated with visible light. The response of the sensor to visible light decreased with increase of operating temperatures. Transient resistance vs. time of the sensor measured during light turns on/off is shown in Figure S10 (Supplementary), which suggests the possibility of using this device for visible light sensor.

4. Conclusion

We reported the facile synthesis of micro-wheels composed of self-assembled tungsten oxide nanorods for the monitoring of highly toxic Cl_2 gas. Given their robustness, superior characteristics, and simple solution process, the prepared micro-wheels were used as a basis to fabricate a low-cost and effective sensor that satisfies the real-time measurement of ppb level Cl_2 gas for environmental pollution monitoring. The sensor shows a high response of approximately 10 folds to 100 ppb Cl_2 and a low *DL* of 18 ppt. The prepared micro-wheels may be effectively used in photo-catalytic, visible light sensor, electrochemical, and electrochromic applications.

Acknowledgements

This research was funded by the Vietnam National Foundation for Science and Technology Development (Code: 103.02-2014.06) and VLIR-UOS under the Research Initiative Project (ZEIN2012RIP20). Authors thank Dr. Hugo Nguyen for assistance in electrode fabrication.

References

1 R. Das and P. D. Blanc, *Toxicol. Ind. Health*, 1993, **9**, 439–455.

2 C. W. White and J. G. Martin, *Proc. Am. Thorac. Soc.*, 2010, **7**, 257–63.

3 W. Hui, X. Jiaqiang and P. Qingyi, *CrystEngComm*, 2010, **12**, 1280.

4 P. Thi Hong Van, N. Hoang Thanh, V. Van Quang, N. Van Duy, N. Duc Hoa and N. Van Hieu, *ACS Appl. Mater. Interfaces*, 2014, **6**, 12022–30.

5 J. Polleux, N. Pinna, M. Antonietti and M. Niederberger, *J. Am. Chem. Soc.*, 2005, **127**, 15595–601.

6 G. Gu, B. Zheng, W. Q. Han, S. Roth and J. Liu, *Nano Lett.*, 2002, **2**, 849–851.

7 Z. Zhou, B. Kong, C. Yu, X. Shi, M. Wang, W. Liu, Y. Sun, Y. Zhang, H. Yang and S. Yang, *Sci. Rep.*, 2014, **4**, 3653.

8 N. Yamazoe, *Sensors Actuators B Chem.*, 2005, **108**, 2–14.

9 K. Liu, N. Zhao and E. Kumacheva, *Chem. Soc. Rev.*, 2011, **40**, 656–71.

10 H.-K. Kim, S.-H. Park, S.-B. Yoon, C.-W. Lee, J. H. Jeong, K. C. Roh and K.-B. Kim, *Chem. Mater.*, 2014, **26**, 4838–4843.

11 Z. Liu, M. Miyauchi, T. Yamazaki and Y. Shen, *Sensors Actuators, B Chem.*, 2009, **140**, 514–519.

12 A. Ponzoni, E. Comini, G. Sberveglieri, J. Zhou, S. Z. Deng, N. S. Xu, Y. Ding and Z. L. Wang, *Appl. Phys. Lett.*, 2006, **88**, 203101.

13 Y. Li, W. Luo, N. Qin, J. Dong, J. Wei, W. Li, S. Feng, J. Chen, J. Xu, A. A. Elzatahry, M. H. Es-Saheb, Y. Deng and D. Zhao, *Angew. Chem. Int. Ed. Engl.*, 2014, **53**, 9035–40.

14 J. Wang, P. S. Lee and J. Ma, *Cryst. Growth Des.*, 2009, **9**, 2293–2299.

15 D. Xu, T. Jiang, D. Wang, L. Chen, L. Zhang, Z. Fu, L. Wang and T. Xie, *ACS Appl. Mater. Interfaces*, 2014, **6**, 9321–9327.

16 N. Van Toan, N. V. Chien, N. Van Duy, D. D. Vuong, N. H. Lam, N. D. Hoa, N. Van Hieu and N. D. Chien, *Appl. Surf. Sci.*, 2015, **324**, 280–285.

17 A. Chaparadza and S. B. Rananavare, *Nanotechnology*, 2008, **19**, 1–8.

18 F. Bender, C. Kim, T. Mlsna and J. F. Vetelino, *Sensors Actuators B Chem.*, 2001, **77**, 281–286.

19 S. Bai, K. Zhang, L. Wang, J. Sun, R. Luo, D. Li and A. Chen, *J. Mater. Chem. A*, 2014, **2**, 7927.

20 D. Wang, P. Hu, J. Xu, X. Dong and Q. Pan, *Sensors Actuators B Chem.*, 2009, **140**, 383–389.

Figure caption

Figure 1. A design of gas nanosensor based on micro-wheels made of self-assembled tungsten oxide nanorods

Figure 2. (A) sensor chip fabricated on a thermally oxidized silicon substrate; (B)-(D) SEM images of the micro-wheels made of self-assembled tungsten oxide nanorods

Figure 3. Gas-sensing characteristics: (A) transient resistance vs. time; (B) sensor response as a function of Cl_2 concentration; (C) transient response of ; (D) response of the sensor to different concentration of NH_3.

Micro-wheels Composed of Self-Assembled Tungsten Oxide Nanorods for Highly Sensitive Detection of Low Level Toxic Chlorine Gas

Pham Van Tong[1,2], Nguyen Van Duy[1], Nguyen Duc Hoa[1]*, Nguyen Van Hieu[1]*

[1]International Training Institute for Materials Science (ITIMS), Hanoi University of Science and Technology (HUST), Dai Co Viet, Hanoi, Vietnam

[2]Department of Physics, Faculty of Mechanical Engineering, National University of Civil Engineering (NUCE), No. 55, Giai Phong Str., Hanoi, Viet Nam

Figure 1. A design of gas nanosensor based on micro-wheels made of self-assembled tungsten oxide nanorods

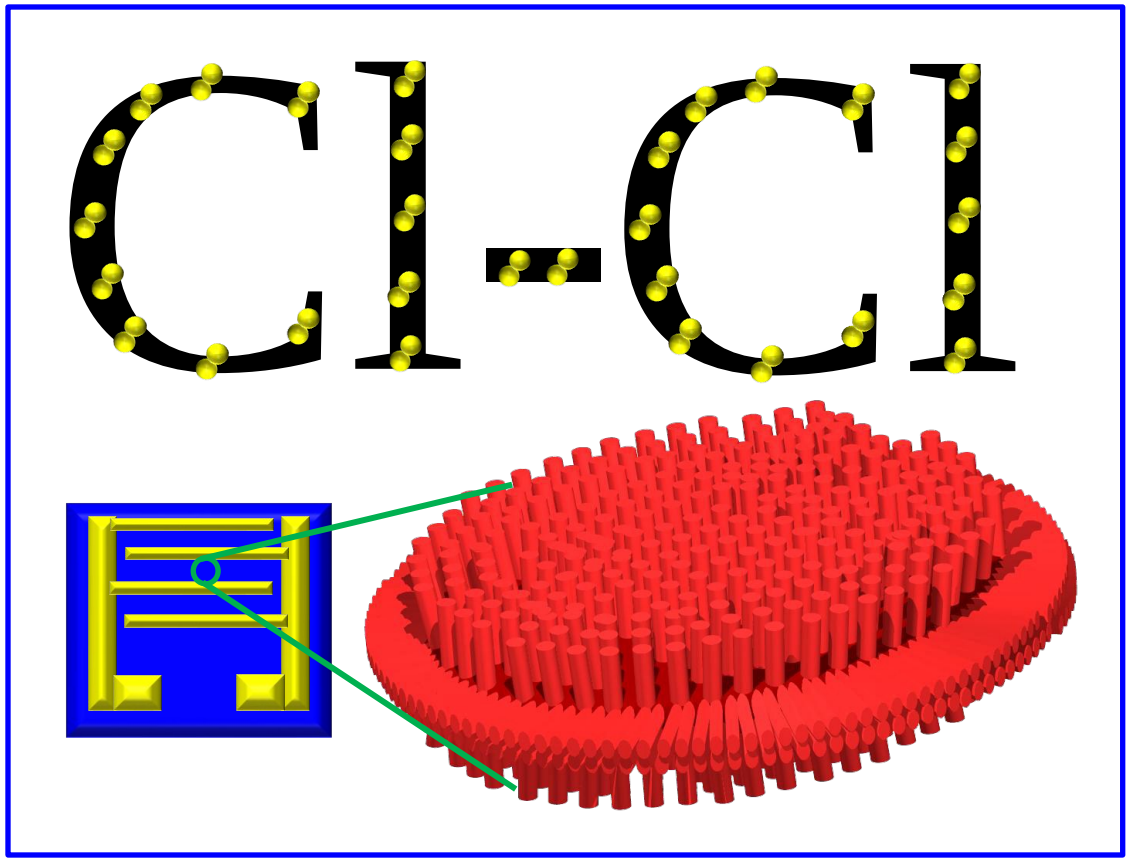

Figure 2. (A) sensor chip fabricated on a a thermally oxidized silicon substrate; (B)-(D) SEM images of the micro-wheels made of self-assembled tungsten oxide nanorods

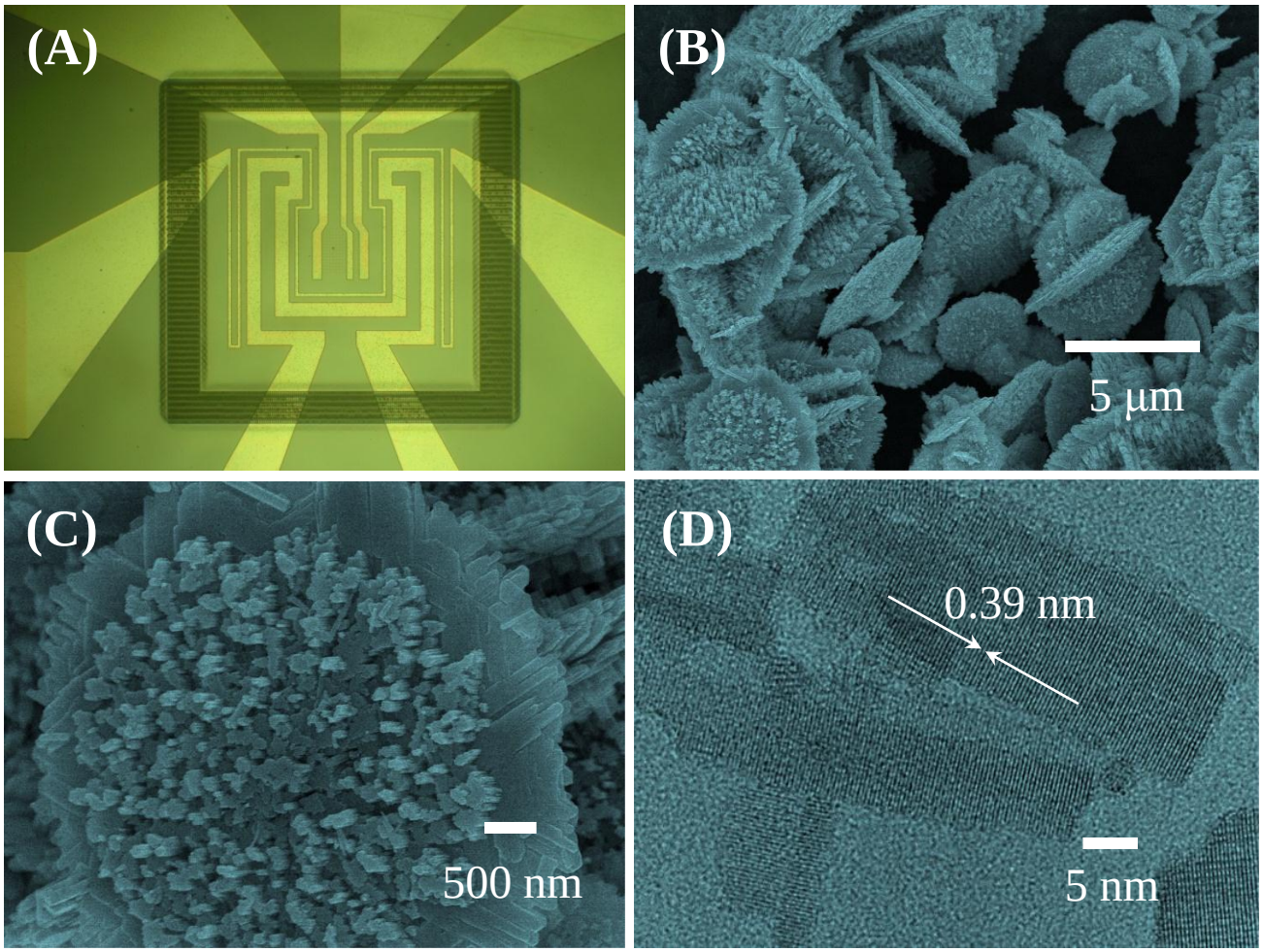

Figure 3. gas-sensing characteristics: (A) transient resistance vs. time; (B) sensor response as a function of Cl_2 concentration; (C) transient response of ; (D) response of the sensor to different concentration of NH_3.

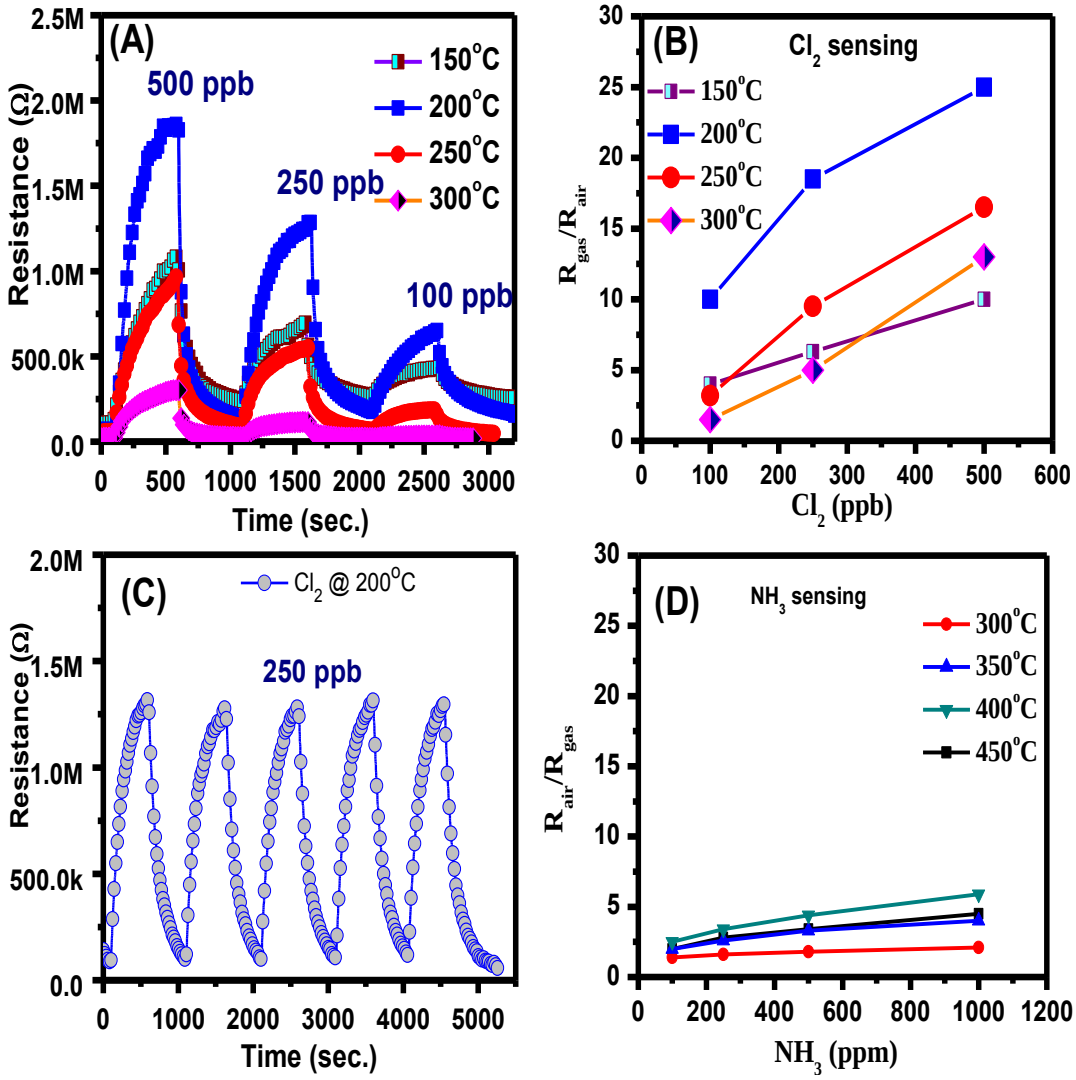

Table of content

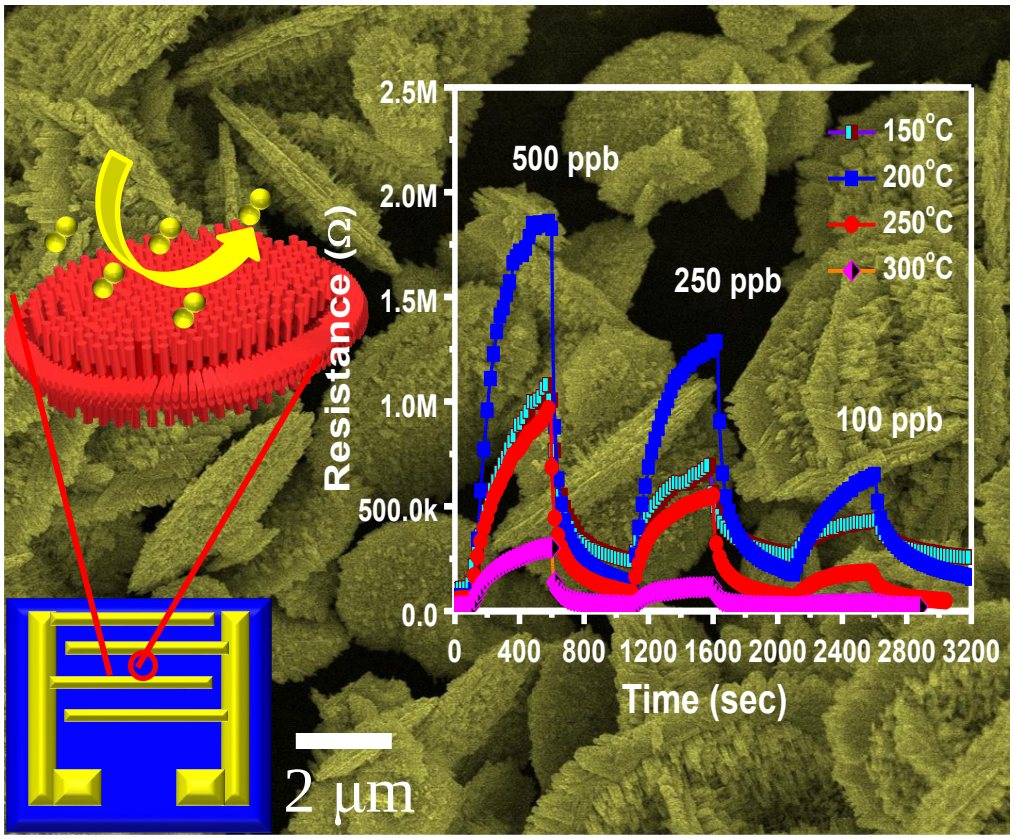

Gas nanosensor based on Micro-wheels composed of self-assembled tungsten oxide nanorods exhibited excellent sensing performance to ppb level Cl_2